Quantum Plumbing Lab (LNQ) internship report

Beatrice Cartocci

July/August 2026

1 Introduction

This report summarises the work carried out during a 6-week-long summer internship in the Quantum Plumbing Lab (LNQ) at EPFL. LNQ studies how quantum-mechanical effects shape the behaviour of liquids confined at the nanometre scale, a regime in which the atomically smooth surfaces offered by two-dimensional (2D) materials such as graphene and hexagonal boron nitride (hBN) are a key experimental tool. The main focus of this internship resides in building the clean, well-characterised 2D-material samples: from mechanical exfoliation to heterostructure assembly.

During the first two weeks, while shadowing another intern, I was taught how to prepare and clean the substrates, how to exfoliate graphite and hBN using tape. Moreover, motivated by the lab's interest in sliding ferroelectricity in twisted hBN, we observed folded hBN flakes, imaging their domain structure by atomic force microscopy (AFM) and Kelvin probe force microscopy (KPFM). In the second part of the internship, I focused on building 2D material heterostructures using deterministic transfers and, in particular, experimenting with mica to achieve a polymer-free transfer. The remainder of this report is organised as follows: Section 2 introduces the theoretical background needed to interpret the samples studied; Sections 3 and 4 present the nano-TM and ferroelectricity objectives in more detail; Section 5 describes the full sample-preparation and heterostructure-assembly methodology; Section 6 analyses and discusses the findings; and Section 7 concludes with the outcomes of the internship and their relevance to the lab's broader research programme.

2 Theoretical background

2.1 2D van der Waals (vdW) materials

Van der Waals (vdW) crystals are layered materials. Within each plane the atoms are strongly bonded together, while the planes themselves are held together only by weak van der Waals interactions. Because this out of plane bonding is so weak compared to the in plane bonding, thin layers of these crystals, down to a single layer in some cases, can be separated from the bulk material: this separation process is called exfoliation and can be done in multiple ways, in this case the exfoliation is always mechanical. Thin layers obtained this way are called 2D materials.

Since the first isolation of graphene in 2004 [1], many other 2D materials have been identified, covering a wide range of electronic behaviour from insulators to semiconductors to conductors [2]. Their properties often differ from those of the same material in bulk form, since reducing a crystal to one or a few atomic layers changes how electrons and light interact within the material. During this internship, three 2D materials were used (as is detailed in the following paragraph): graphene, hBN and mica.

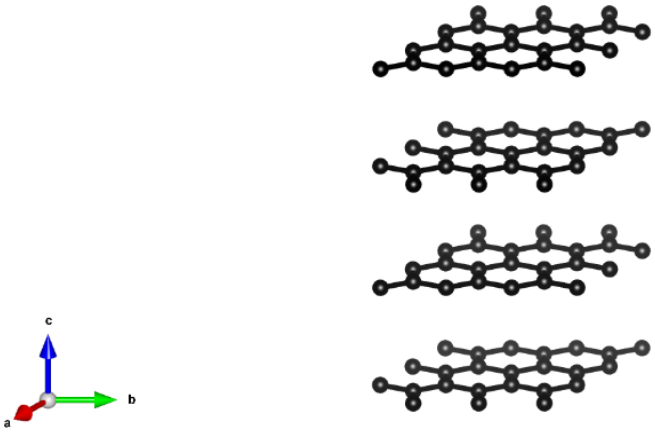

Figure 1: Side view of a layered van der Waals crystal. Atoms are covalently bonded within each plane, while consecutive planes are held together only by weak van der Waals interactions.

2.2 Studied materials

Graphene is a single layer of carbon atoms arranged in a hexagonal, honeycomb pattern, where each atom is bonded to three neighbours. It corresponds to one individual plane of graphite. In practice, the term "graphene" is often used loosely to also describe samples that are a few layers thick, not strictly a monolayer, since the properties stay close to those of true monolayer graphene up to a few layers before starting to resemble bulk graphite.

Hexagonal boron nitride (hBN) has essentially the same hexagonal lattice as graphene, but with alternating boron and nitrogen atoms instead of carbon. This is why it is sometimes called "white graphene." The main difference is electronic: while graphene is a good conductor, hBN is an insulator, which makes it commonly used as a substrate or spacer for other 2D materials.

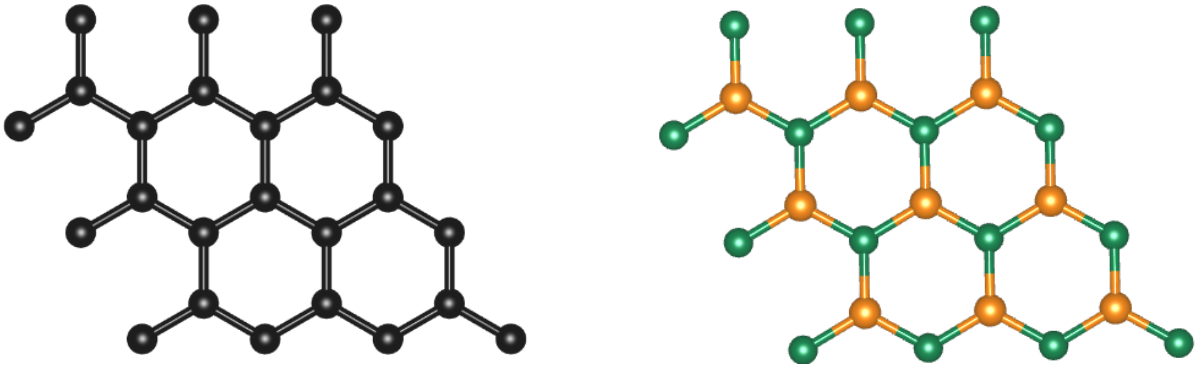

(a) Graphene **(b)** Hexagonal boron nitride

Figure 2: In-plane view of the two honeycomb lattices used in this work. In hBN the two sublattices are occupied by boron and nitrogen atoms instead of carbon.

3 Slip length

One of the lab's focuses is on measuring the slip length of water on various hBN and graphene-based samples using a tuning fork nano-TriboMeter (nano-TM). Slip length, $b = \eta/\lambda$, describes the ratio between a fluid's viscosity and the interfacial friction factor, capturing how far the boundary condition deviates from the classical no-slip case. By preparing and characterizing 2D material samples of varying thickness and substrate, and probing them with the nano-TM, the aim is to extract slip length values and identify how they depend on these structural parameters.

This contributes to a broader understanding of nanoscale fluid-solid interactions, with relevance to nanofluidic applications such as water filtration, desalination, and low-friction fluid transport, where the atomically smooth surfaces of 2D materials offer potential for significantly enhanced flow performance.

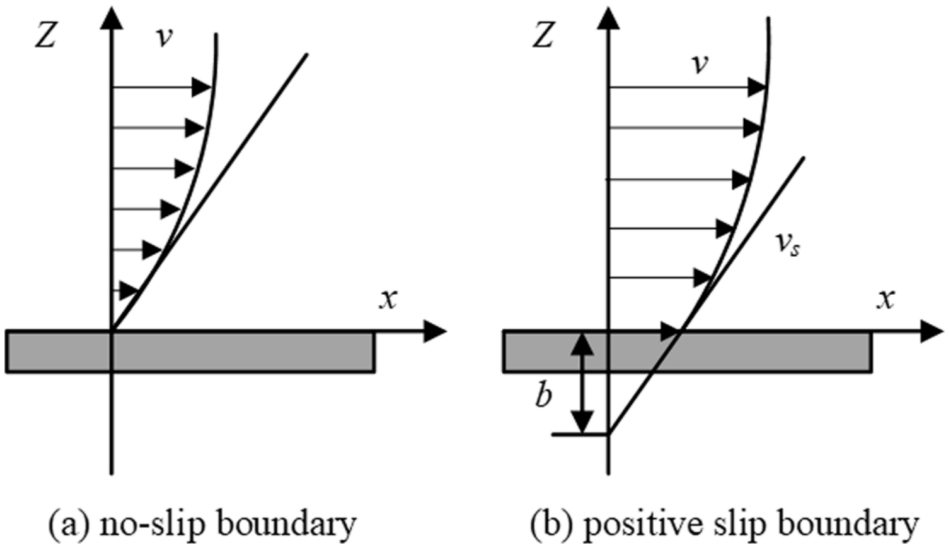

Figure 3: Velocity profile of a fluid at a solid wall for (a) the classical no-slip boundary condition and (b) a positive slip boundary condition, where the extrapolated profile vanishes a distance b inside the solid.

4 Ferroelectricity

Ferroelectricity is a material property where a substance has a built-in electric polarization that can be reversed by applying an external electric field. This polarization comes from a shift in the positions of positive and negative charges within the crystal, and the ability to switch it back and forth is what makes ferroelectric materials unique. For ferroelectricity to occur, the crystal structure must lack a center of symmetry; otherwise, any local dipoles would cancel each other out and no net polarization would remain.

In its bulk form, hexagonal boron nitride has an antiparallel stacking arrangement called AA′, where the layers are positioned so that nitrogen atoms align above boron atoms and vice versa. This configuration preserves a center of symmetry, which means the bulk material has no spontaneous polarization and is therefore not ferroelectric. However, ferroelectricity does appear when the stacking is changed. In a bilayer of hBN with parallel orientation, the layers can be arranged in two ways: AB stacking, where a boron atom sits directly above a nitrogen atom, or BA stacking, where a nitrogen sits above a boron. Both of these arrangements break inversion symmetry, and they create electric dipoles that point in opposite directions out of the plane. The dipole forms because nitrogen attracts electrons more strongly than boron does, and when a nitrogen from one layer aligns with a boron from the other, the electron cloud distorts and generates a net charge separation.

If the two layers are twisted by a small angle θ, the resulting moiré superlattice contains alternating regions of AB and BA stacking, arising from the periodic misalignment between layers. The moiré periodicity λ is related to the twist angle by

$$\lambda = \frac{a}{2\sin(\theta/2)}, \tag{1}$$

where a is the lattice constant , meaning that as θ increases, the ferroelectric domains (AB and BA regions) shrink in size. The hexagonal pattern that emerges is a signature of interface

reconstruction: the AA-stacked regions are energetically unstable and shrink as the material relaxes, giving rise to the characteristic triangular domain shapes observed experimentally.

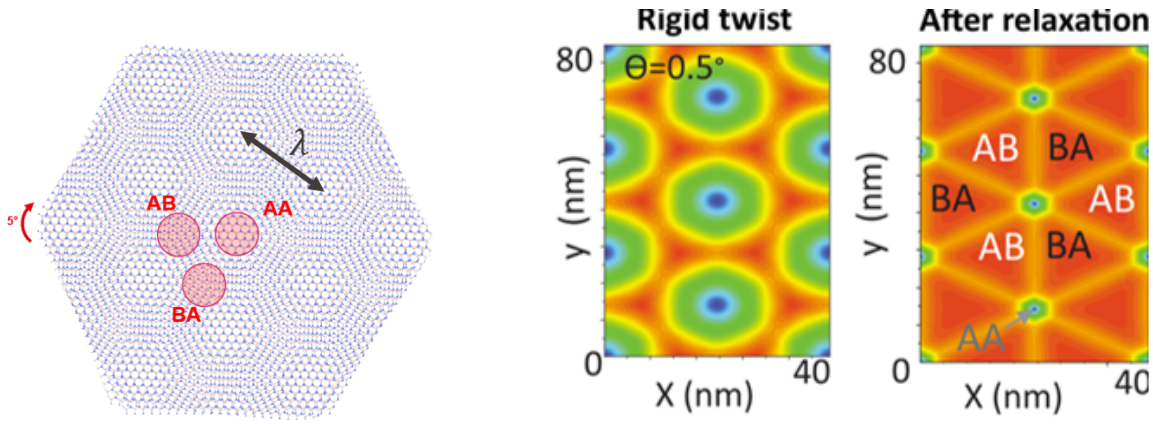

(a) Moiré superlattice **(b)** Rigid twist vs. relaxed structure

Figure 4: (a) Moiré pattern formed by two hBN layers twisted by a small angle, showing the AA, AB and BA stacking regions and the moiré periodicity λ (adapted from [5]). (b) Calculated domain structure for a $\theta = 0.5°$ twist before and after relaxation: the AA regions shrink and triangular AB/BA domains form (adapted from [3]).

When an electric field is applied, the layers slide slightly relative to each other, switching these regions from one stacking type to the other. This process, known as sliding ferroelectricity, is why ferroelectric behavior can be observed in hBN bilayers even though the bulk material is not ferroelectric.

4.1 Characterizing ferroelectric BN by AFM and KPFM

Once a suitable BN-based sample was assembled, its ferroelectric character was probed using atomic force microscopy (AFM), a technique that maps surface height variations by scanning a sharp tip mounted on a flexible cantilever across the sample. A laser reflected off the back of the cantilever onto a photodetector tracks its deflection as the tip moves over the surface, allowing the topography to be reconstructed with nanometre-scale resolution. Measurements were performed in tapping mode, where the cantilever is oscillated near its resonance frequency and changes in that oscillation, caused by variations in surface height or local surface properties, are recorded as the tip scans across the sample.

This technique was applied to a folded hBN flake, a configuration in which a single sheet is folded back on itself to naturally create both AB and BA stacked regions side by side, separated by domain boundaries. While the AFM topography reveals the physical structure of the fold and any wrinkles or steps in the material, it does not on its own distinguish between the different stacking domains, since AB and BA regions are essentially flat and indistinguishable in height.

To resolve this, the same regions were also imaged using Kelvin probe force microscopy (KPFM), which maps variations in surface potential rather than height. Because AB and BA stacking domains carry opposite out-of-plane spontaneous polarization, they produce a measurable difference in local surface potential, allowing KPFM to directly visualize the ferroelectric domain pattern that AFM alone cannot distinguish. The resulting maps reveal the triangular domain structure expected from the moiré superlattice, with contrast between adjacent regions corresponding to the alternating AB/BA stacking and the boundaries where the polarization switches sign. Together, AFM and KPFM provide a complementary picture of the sample: AFM confirms the physical geometry of the fold and the presence of the moiré-related structure, while KPFM directly images the underlying ferroelectric domains, making it possible to correlate the size and shape of the AB/BA regions with the local twist angle predicted by Eq. (1).

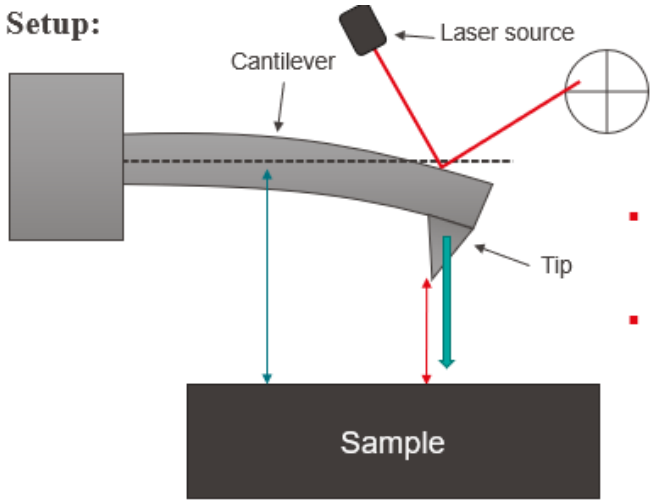

Figure 5: AFM setup: a laser is reflected off the back of the cantilever onto a photodetector, which tracks the deflection of the tip as it scans the sample.

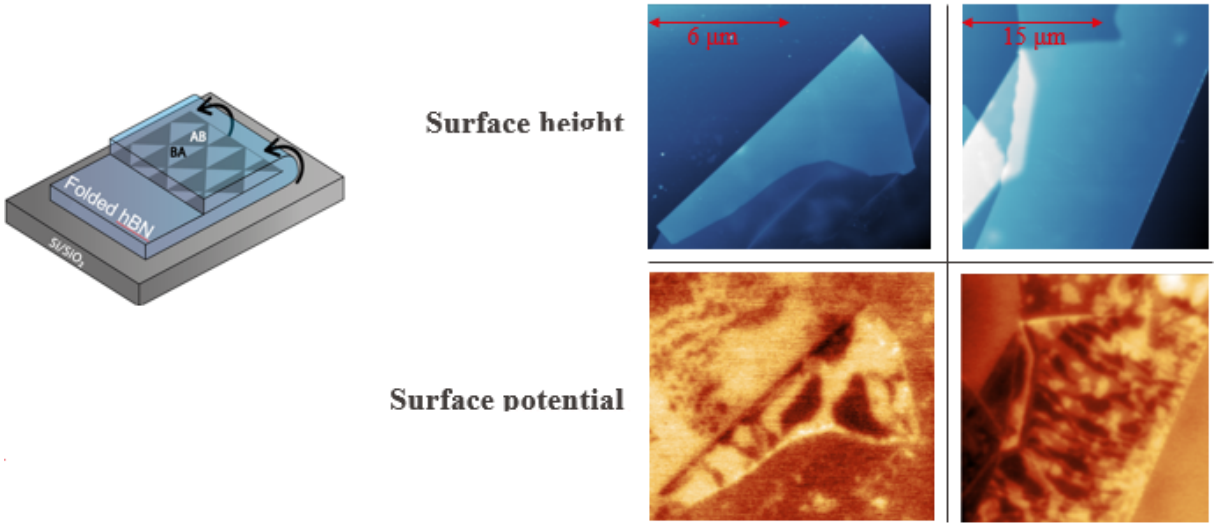

Figure 6: Folded hBN flake on SiO_2/Si (schematic adapted from [5]). Top: AFM surface height maps, which reveal the geometry of the fold but not the stacking order. Bottom: KPFM surface potential maps of the same regions, where the triangular AB/BA ferroelectric domains become visible.

5 Sample preparation

5.1 Substrate preparation and cleaning

Samples are fabricated on Si chips coated with 280–300 nm of SiO_2, cut from larger wafers into roughly 1 cm × 1 cm squares. The wafer is first scored with a diamond pencil at regular intervals on the oxide side, then snapped along these marks using a glass slide to produce strips, and the same process is repeated in the perpendicular direction to obtain individual chips. Before exfoliation, each chip is cleaned by two successive 5-minute ultrasound baths in acetone followed by one in isopropanol, drying with N_2 between steps to avoid leaving residues. Chips destined for a PVC-stamp transfer are then exposed to oxygen plasma for 3 minutes (∼0.5 bar O_2 pressure, 100% power, i.e. ∼200 W) to remove any remaining organic contamination and to improve flake adhesion during exfoliation; because this surface activation only lasts for a limited time, exfoliation is carried out immediately afterwards. Chips intended for a mica-stamp transfer skip this plasma-cleaning step entirely.

5.2 Exfoliation

Flakes of hBN and graphene are obtained through mechanical exfoliation using tape, performed immediately after the plasma-cleaning step for best results. Either Magic Tape "Greener" (stickier) or a blue exfoliation tape (less sticky, and therefore preferred when tape residue must be minimised) can be used.

For hBN, small crystals are placed on a strip of tape and folded/peeled repeatedly until a thin, even layer of material coats the tape. A promising region, dense in flakes but not too thick, is then pressed onto the chip and held under pressure for at least 30 seconds before slowly peeling the tape away, adjusting the peeling angle to control flake thickness (a shallower angle favours thinner flakes). Graphene exfoliation follows a similar logic but starts from a graphite crystal, going through a "mother tape" and then "daughter tapes" made from it; a daughter tape is only used once a sufficiently dense and grey region is visible by eye. The tape is then pressed onto the chip, heated briefly at 100°C to improve adhesion, and peeled off slowly.

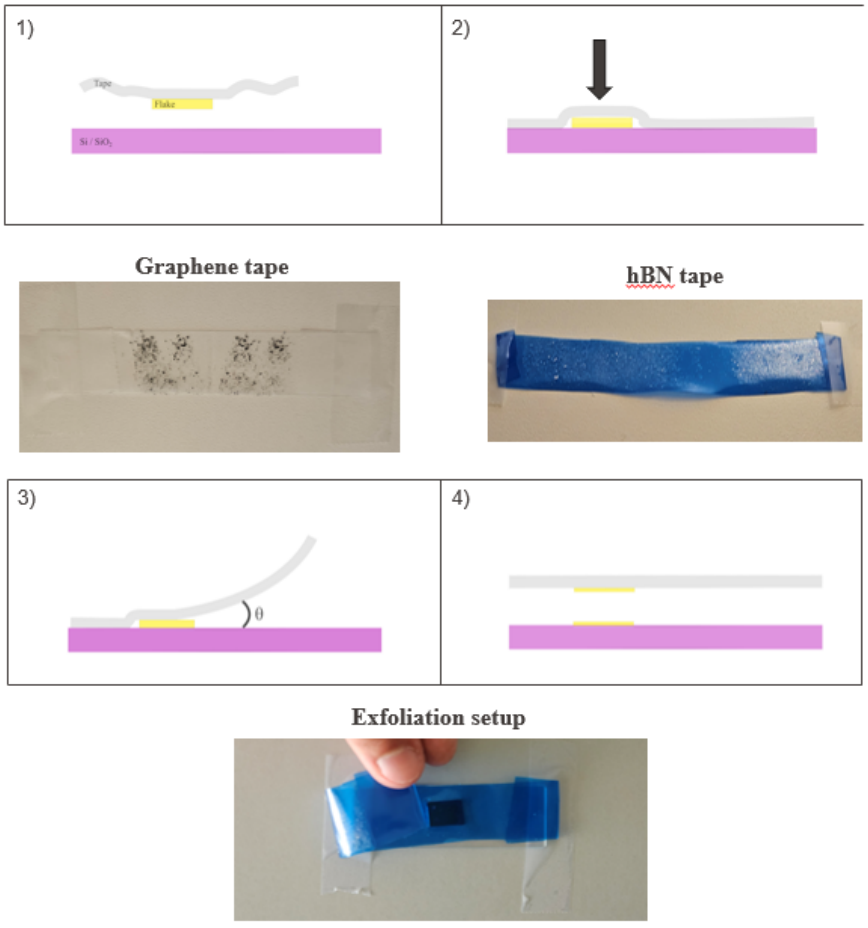

Figure 7: Mechanical exfoliation. Steps 1–2: the flake-coated tape is brought into contact with the SiO_2/Si chip and pressed down. Steps 3–4: the tape is peeled away at a controlled angle θ, leaving flakes on the chip. Photographs: graphene and hBN tapes, and the exfoliation setup (scheme and photographs from [9]).

5.3 Flake identification and thickness estimation

Once exfoliated, flakes are identified and their thickness estimated by optical contrast. Both hBN and graphene show characteristic, periodic colour changes with thickness under the microscope: thin hBN appears blue and becomes increasingly hard to distinguish from the substrate as it gets thinner, while graphene monolayers appear as a faint blue that is barely visible due to the

low contrast with SiO_2, becoming greenish and then yellow as the flake thickens. As a rough guide, graphene flakes with a more intense blue colour are approximately 10–30 nm thick, with thicker flakes turning greenish and finally yellow (yellow flakes can range anywhere from ∼60 nm to ∼500 nm, so colour alone is ambiguous in that regime). For hBN, blue flakes are typically thinner than 20 nm, green ones 20–50 nm, yellow ones 50–90 nm, and reddish ones ∼100 nm thick; because this colour progression is periodic, flakes around 140 nm again appear greenish, so care must be taken not to confuse a thick flake for a thin one.

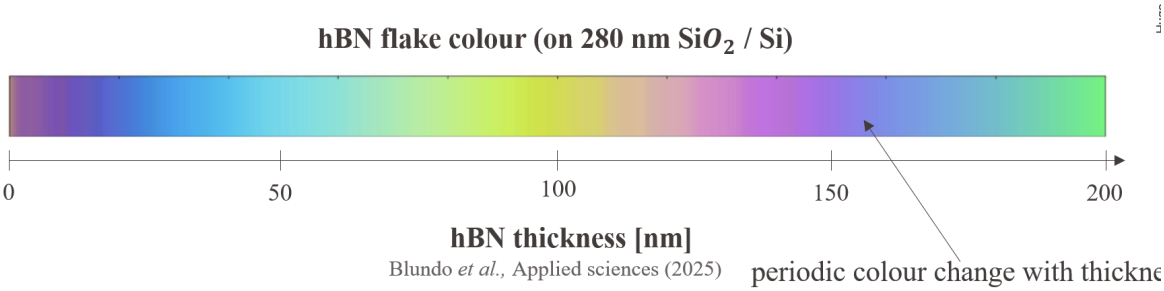

Figure 8: Periodic variation of the apparent colour of an hBN flake on 280 nm SiO_2/Si as a function of its thickness (adapted from [4]).

Because colour alone only gives a rough estimate, flake thickness is also evaluated more quantitatively using the software Slopey, which compares the light intensity of the flake to that of the surrounding substrate. This is done through the contrast factor and the flake-to-substrate intensity ratio, from which a slope value is extracted and compared against a calibration curve relating slope to number of layers.

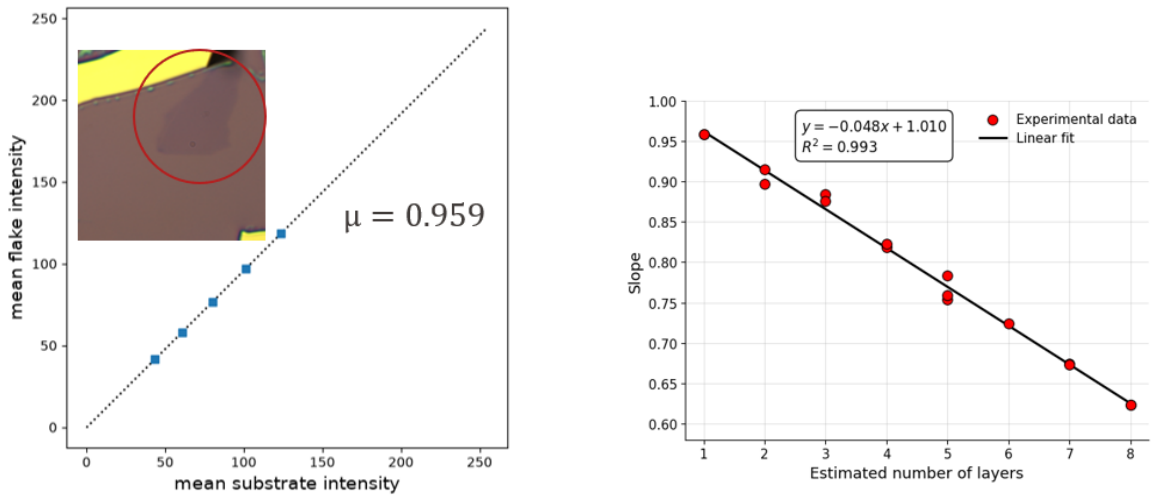

(a) Slope extraction

(b) Calibration curve

Figure 9: Thickness estimation with Slopey. (a) Mean flake intensity plotted against mean substrate intensity over several colour channels; the slope μ of the linear fit characterises the flake. (b) Calibration of the slope against the estimated number of layers.

Using this combined approach (colour and Slopey analysis), suitable flakes of both graphene and hBN were identified and selected for the transfer process.

5.4 Heterostructure assembly: PVC and mica stamps

Heterostructures are assembled using a home-made stamp that picks up flakes and stacks them before depositing the final structure onto a clean substrate (or alternatively picks up a flake and

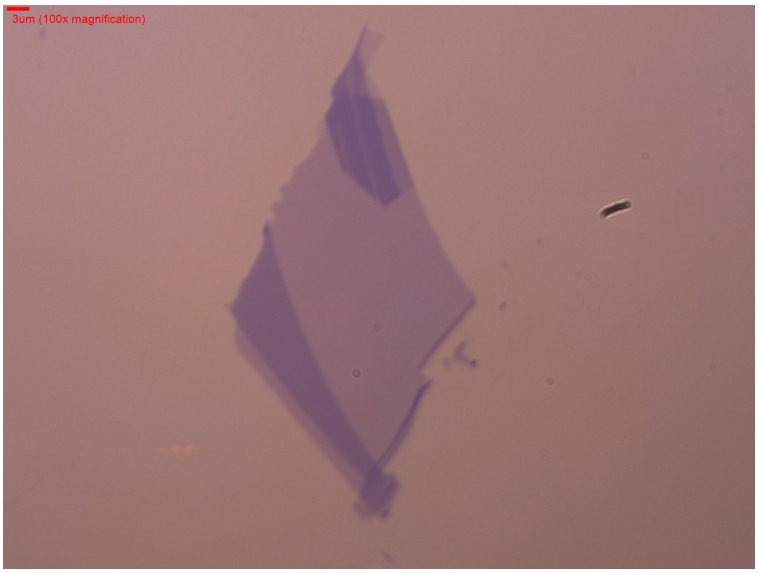

Figure 10: Optical micrograph (100× magnification) of a selected flake; the scale bar corresponds to 3 µm.

deposits it on top of another flake). Two stamp technologies were used : a polymer (specifically PVC) film on PDMS, and a polymer-free one using a muscovite-mica membrane on PDMS.

Muscovite mica is a layered aluminosilicate that cleaves readily along its basal planes, so a fresh piece of tape can peel off a thin, transparent sheet that is flat down to the atomic scale over large areas. Unlike graphene and hBN, its layers are not held together by van der Waals forces alone but by interlayer potassium ions, which makes the membrane considerably stiffer than a polymer film and limits how thin it can be made. The property that matters here is that a freshly cleaved mica surface is both clean and atomically flat, and that mica is a crystal rather than a polymer, so it leaves no polymeric residue on the flakes it touches.

The two share the same substrate preparation, exfoliation and flake-identification steps described above; where they differ is in how the stamp itself is built and in the temperatures used for pick-up and deposition.

Polymer-free, mica-based assembly of 2D heterostructures is a very recent development: at the time of the internship it has been demonstrated in only a single publication, from 2026 [6], so there was very little prior practical guidance to draw on. Reproducing the method therefore required substantial trial and error to arrive at a stamp-fabrication procedure and a set of pick-up/deposition temperatures that worked reliably in this setup. As detailed below, the resulting success rate is somewhat lower than for the well-established PVC stamp, but the technique does work, and reliably yields heterostructures once the procedure is followed.

5.4.1 Stamp fabrication

Both stamps consist of a small PDMS cube (0.5 cm × 0.5 cm), placed ∼1 cm from the edge of a glass slide.

For the **PVC stamp**, we start by placing the PDMS cube. Then, a PVC film is stretched from its box across a table edge and a glass slide is slid underneath and stuck to the back of the film, keeping it taut and free of folds. A precise ∼1.5 cm × 1.5 cm square of PVC , roughly twice the size of the PDMS cube , is then cut out on the glass slide. A hole larger than the PDMS cube is punched in a piece of Magic Tape, which is used to pick up the PDMS cube so that the hole is fully covered by the PVC square; the hole is aligned with the cube, the tape is fixed all around it, and the excess PVC and tape are trimmed away with a laboratory knife (Fig. 11).

For the **mica stamp**, the cube is cut from a thinner, ∼1 mm PDMS gel. A polygon-shaped

hole , sized to be larger than the PDMS cube but smaller than the mica stack, typically around 0.8 cm, and cut without sharp angles ($< 90°$) to prevent the tape from ripping , is cut into two stacked layers of Magic Tape. This double layer of tape is then pressed onto a bulk mica crystal and peeled off to exfoliate a thin mica sheet across the hole. The mica-covered tape is placed over the PDMS square, with two extra pieces of tape added at the top and bottom to seal out air pockets between the mica and the PDMS, and any excess tape is trimmed from the sides with a laboratory knife (Fig. 12). Because the first mica flake exfoliated from a given crystal has typically been in contact with air the longest, it is discarded, and the mica is exfoliated once more with a fresh piece of tape immediately before use, to keep the stamp surface as flat and clean as possible. Because mica is a naturally cleavable, atomically flat crystal rather than a polymer film, this approach avoids the polymer residues that can be left behind by PVC-based transfers, making it attractive for cleaner, polymer-free heterostructure assembly.

Figure 11: The PDMS/PVC stamp used for pick-up and transfer. Left: the tools and materials used to assemble the stamp (glass slide, PDMS cube, PVC film, scalpel, tweezers and a hole punch). Right: close-up of the finished stamp, showing the PDMS square exposed through the hole cut in the PVC film [9].

Figure 12: Mica-based stamp: a thin muscovite mica membrane (dashed box) is exfoliated across a polygonal hole cut into two stacked layers of tape and placed over the PDMS cube, with extra tape sealing the edges to keep out air pockets

5.4.2 Flake pick-up

Pick-up is done under the microscope, with the stamp mounted above a heated stage that holds three chips over vacuum holes; with the vacuum switched on to hold the chips flat, the stamp is first set in a "position" mode to locate the flake of interest, before switching to an "under the microscope" mode in which the membrane is aligned with the flake and slowly lowered into contact (Fig. 13). For the **PVC stamp**, the stage is held at 70°C, the contact line is advanced slowly and smoothly over the flake, and the stamp is held in place for around 30 seconds once past the flake before being carefully retracted , a successful pick-up is confirmed when the flake changes colour and appears greyish once transferred onto the stamp. The **mica stamp** behaves rather differently at this stage: the stage is held at a higher 80–90°C, and since mica is rigid rather than flexible, the contact line advances irregularly rather than sweeping smoothly across

the flake, with small impurities on either the substrate or the mica surface locally pinning the contact and leaving much larger uncontacted "holes" than typically seen with the polymer stamp; the contact is then retracted gently, but not too slowly. Unlike PVC, mica also cannot pick up graphene directly from the bare substrate , a top hBN flake must already be present on the stamp to serve as the pick-up surface for graphene. If a pick-up fails for either stamp, it is generally worth trying again at a slightly shifted stamp position and a somewhat higher temperature (90–95°C for mica, 85°C for PVC).

In short, mica is far less flexible than the PVC film, so its contact line advances irregularly and pins on impurities, making mica transfers harder to achieve reliably. However, being a crystal rather than a polymer film, mica leaves much less residue on the finished heterostructure than a polymer stamp does, which is precisely what makes the extra effort worthwhile, as confirmed directly by AFM.

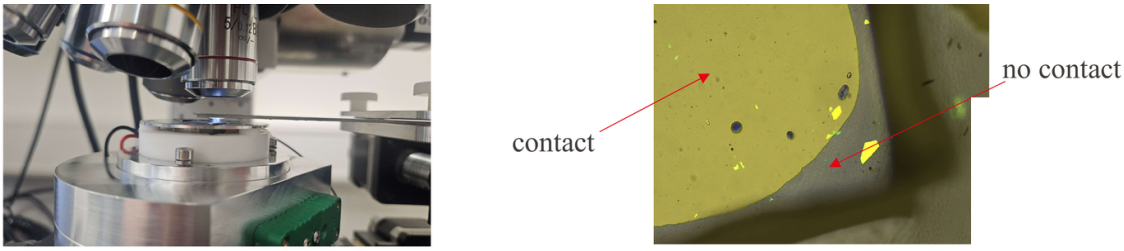

Figure 13: Pick-up under the microscope. Left: the sample stage and stamp positioned above it during a pick-up. Right: optical image of the stamp approaching a flake, with the contact line between the stamp and the chip visible; regions already in contact appear darker (arrow, "contact"), while the flake not yet reached by the contact line remains unaffected ("no contact") [9].

5.4.3 Heterostructure formation and deposition

To build a heterostructure, a second flake is picked up in exactly the same way as above, this time carefully aligning it with the flake already sitting on the stamp (Fig. 14).

Once the desired stack has been assembled, it is deposited onto a new, clean substrate by bringing the stamp into contact again, this time with the temperature raised in order to favour flake–substrate adhesion over flake–membrane adhesion. For the **PVC stamp**, the temperature is raised to 130°C; a successful deposition is confirmed when the flake recovers its original colour as the stamp is retracted, though some polymer residue can still be left behind on the contact area. Deposition with the **mica stamp** differs in one important respect: unlike PVC, mica cannot release a flake directly onto a bare substrate, since the adhesion between mica and the flake isn't weak enough compared to the adhesion between the flake and the substrate. Release only works onto another flake already present on the chip, typically a bottom hBN layer, and deposition temperatures are correspondingly higher (120–180°C). During this step, the mica is also not brought into full contact with the bottom flake , a small uncontacted region is deliberately left to avoid accidentally picking the bottom flake back up.

Following this procedure, both graphene-on-BN and BN-graphene-BN heterostructures were successfully assembled with each stamp.

6 Findings

The two stamps differed both in how easily they could be used and in the surfaces they left behind.

The mica stamp was the harder of the two to work with. The membrane is fragile, and it often broke while the stamp was being made, so a number of attempts ended before any transfer could be attempted. Contact with the substrate was also less homogeneous than with the polymer

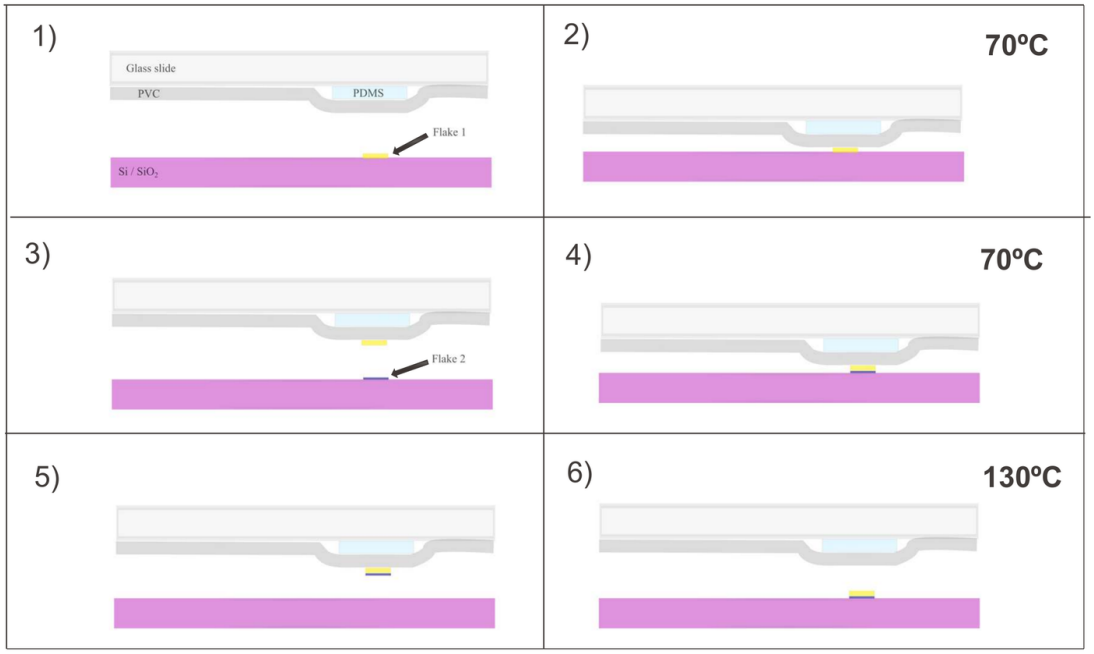

Figure 14: Six-step hot pick-up and deposition sequence used to build a heterostructure. Steps 1–2: flake 1 on the substrate is picked up by bringing the stamp into contact at 70°C. Steps 3–4: the stamp, now carrying flake 1, is aligned with flake 2 on a second substrate and the two are picked up together, again at 70°C. Steps 5–6: the assembled stack is brought into contact with a new, clean substrate and released at 130°C, completing the deposition [9].

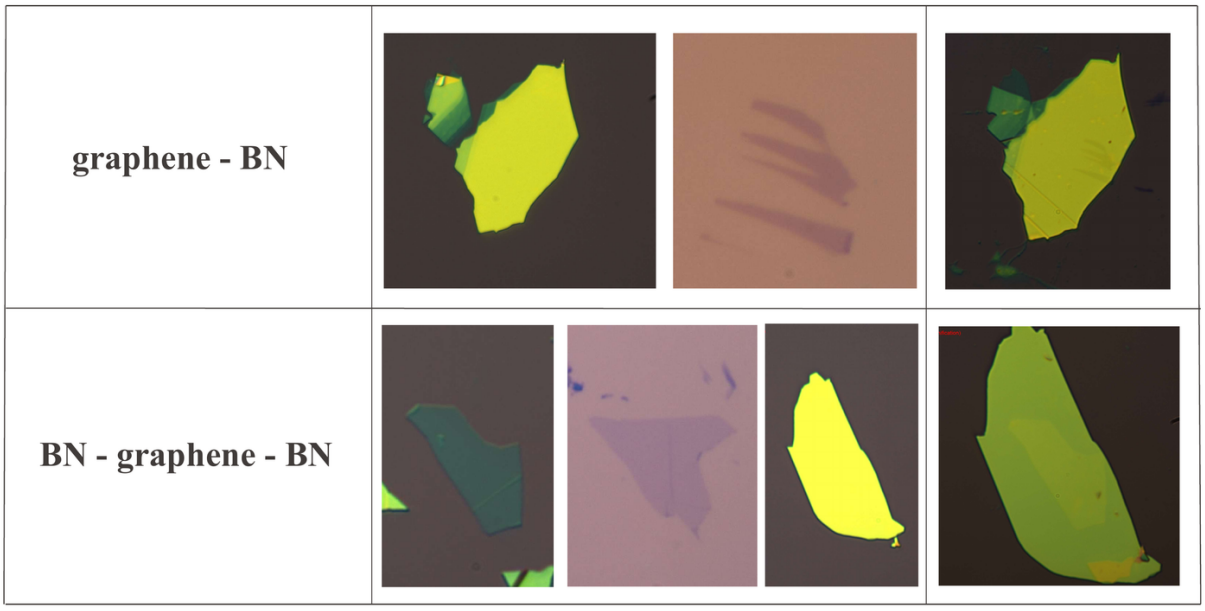

Figure 15: Assembled heterostructures.

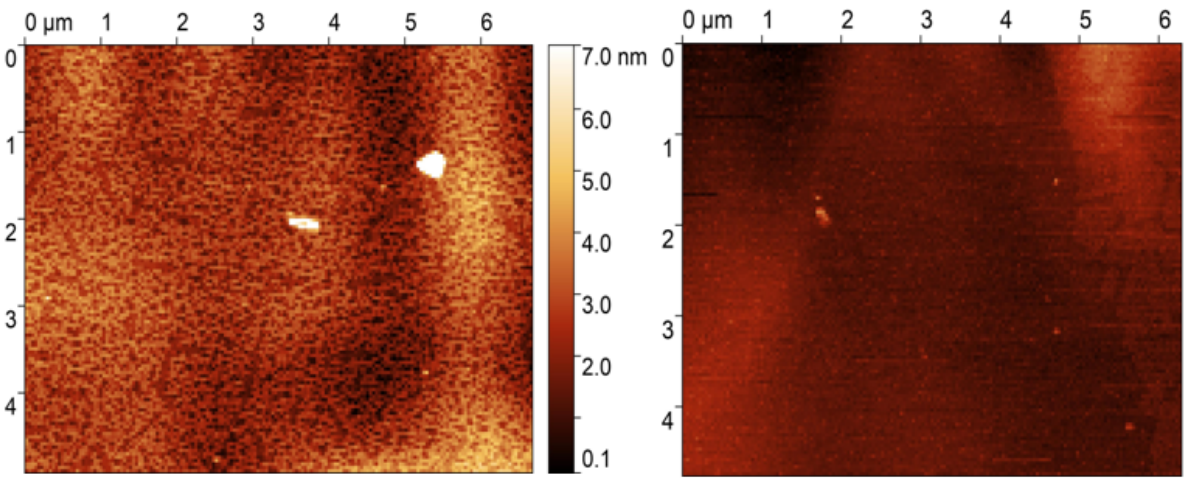

Figure 16: AFM scan of a heterostructure built using a PVC (left) and mica (right) stamp

stamp, with some regions touching down while others stayed lifted, which made the transfer less predictable. Flakes tended to stick less readily to mica as well, so pick-up failed more often. Taken together, these three factors gave the mica route a noticeably lower success rate.

However, it gives a better result in terms of cleanliness of the surface. Mica is a naturally cleavable, atomically flat crystal rather than a polymer film, so it leaves far less residue on the sample. The atomic force microscopy scans in Figure 16 show this directly. The heterostructure assembled with the PVC stamp carries a mottled texture spread across the whole scan area, consistent with polymer residue left at the interface, while the one assembled with mica is largely uniform over comparable areas, with only a few isolated particles and some gentle long-range variation. Since the slipperiness of the wall is measured at the interface itself, that difference is worth the extra difficulty, and it is the main argument for continuing to develop the mica route rather than defaulting to the polymer one.

7 Conclusion

Over the six weeks of this internship, a full sample-preparation route was set up and carried through: substrate cleaning, mechanical exfoliation of graphite and hBN, thickness identification by optical contrast and Slopey analysis, and heterostructure assembly by deterministic transfer. Both graphene-on-BN and BN-graphene-BN stacks were successfully assembled with each of the two stamp technologies.

The main outcome concerns the polymer-free route. Starting from a single published demonstration, a working mica-stamp procedure was established: a mica membrane exfoliated across a polygonal hole in two stacked layers of tape over a thin PDMS cube, pick-up at 80–90°C (retried at 90–95°C on failure), and deposition at 120–180°C onto a flake already present on the chip rather than onto bare substrate, with graphene requiring a top hBN flake on the stamp to be picked up at all. The success rate remains below that of the well-established PVC stamp, mainly because the membrane is fragile and the rigid contact line advances irregularly, but the procedure is reproducible once followed.

AFM confirms what motivates this extra difficulty: the mica-assembled heterostructure shows a largely uniform surface with only isolated particles, while the PVC-assembled one carries a mottled texture consistent with polymer residue across the whole scan. Since the nano-TM measures slip length at the solid–liquid interface itself, residue at that interface directly limits how far the measured values can be trusted. The mica route is therefore worth continuing to develop for the lab's nanofluidic measurements, with the fragility of the membrane and the pick-up success rate as the natural next targets for improvement.

Acknowledgements

I am very grateful to Prof. Kavokine for the opportunity to intern in his lab, to Jules Fraunié, my supervisor, for all his time, guidance and advice, and to all the members of the lab for answering my questions and for being so kind and welcoming.

References

[1] K. S. Novoselov *et al.*, *Electric field effect in atomically thin carbon films*, Science **306**, 666–669 (2004).

[2] K. S. Novoselov, A. Mishchenko, A. Carvalho and A. H. Castro Neto, *2D materials and van der Waals heterostructures*, Science **353**, aac9439 (2016).

[3] M. Vizner Stern *et al.*, *Interfacial ferroelectricity by van der Waals sliding*, Science **372**, 1462–1466 (2021).

[4] E. Blundo *et al.*, *Identification of hexagonal boron nitride thickness on SiO_2/Si substrates by colorimetry and contrast*, Applied Sciences **15**, 8400 (2025).

[5] J. Fraunié, *PhD thesis* (2025).

[6] I. Babich *et al.*, *Polymer-free van der Waals assembly of 2D material heterostructures using muscovite crystals*, Nature Communications **17**, 6017 (2026).

[7] A. Lizée *et al.*, *Slip length measurement on 2D materials with a tuning-fork nano-TriboMeter*, arXiv preprint (2024).

[8] Y.-Z. You, *Moiré Superlattice*, You Group @ UCSD, https://everettyou.github.io/2018/05/21/Moire.html (2018).

[9] H. Praz, *Internship Presentation*, Quantum Plumbing Lab (LNQ), EPFL (2026).